An experimental investigation on ultra-precision instrumented smart aerostatic bearing spindle applied to high speed micro-drilling

Chao Wang[a, *]

c.wang.1@warwick.ac.uk

Kai Cheng[b]

Richard Rakowski[b]

Juliette Soulard[a]

[a]Warwick Manufacturing Group (WMG), The University of Warwick, Coventry CV4 7AL, UK

[b]Advanced Manufacturing and Enterprise Engineering (AMEE), College of Engineering, Design and Physical Sciences, Brunel University London, Uxbridge UB8 3PH, UK

*Corresponding author.

Abstract

High speed drilling of small diameter holes ranging from 0.1 to 1 mm in printed circuit board (PCB) drilling industry has been largely carried out by using tungsten carbide twist drills and high speed spindles. In high speed drilling, however, the tool wear leads to increased cutting forces and results in poor hole quality as well as the hole location inaccuracy. Both hole quality and location accuracy are further considered as significant issues in drilling multilayer and heavy copper layered PCB workpieces. This paper presents the experimental development of an instrumented smart spindle, which can examine the tool wear by measuring the axial shaft displacement (known as the axial displacement) on the fly and thus applicable to real-time drilling processes. Cutting trials using the instrumented smart spindle and a Kistler dynamometer (9345A) on the customized multilayers PCB workpiece have shown a good correlation between the axial displacement and axial drilling force measurements. The axial displacement is capable of being used to detect the drilling engagement with each copper layer. Furthermore, the instrumented smart spindle can additionally be used to prevent a thrust bearing from being over-loaded and most importantly to detect tool wear in process.

Keywords: High speed drilling; Aerostatic bearing spindle; Micro tool wear; Instrumented smart spindle; Multilayer PCB drilling

1 Introduction

High speed drilling is one of the most essential and efficient ways in processing printed circuit boards (PCB) for connecting two or more layers electronically. In order to mechanically drill small holes with corresponding optimal chip loads, high spindle speeds, extensively adopted in the PCB drilling industry, play a pivotal role in the PCB drilling process using tungsten carbide drills. Therefore, from the early days in circuit board manufacture, only air bearing technology offered the capability of attaining very high rotational speeds over long periods of unsupervised operation [1,2].

With the rapid development of the electronics industry, multilayer and heavy copper layer PCB workpieces are becoming more demanding with increasing functionality, high space efficiency, number of wiring layers and higher density of printed circuit components [3]. As the on-board hole density and the layer count increase, there is a real industry requirement for a high registration accuracy of the individual layers and for control of micro holes position and quality. Therefore, a tool wear monitoring system is becoming an essential part of high speed drilling and can prevent tool breakage, excessive burr formation and even the catastrophic failure of aerostatic bearing spindles. In order to avoid such damaging issues, some devices have been specially designed and applied to measure cutting forces. However, the commercial available cutting force measurement devices, namely dynamometers, are not extensively adopted in industrial machining due to their size and weight, applicability to all layout-constrained machines, their interfere with cutting performance because of the stiffness reduction on the machining system, and their substantial costs. Moreover, dynamometers hit the technological bottleneck, i.e. the limited bandwidth and, hence, they are unable to be applied in high speed drilling yet [4–6]. For high speed drilling particularly on multilayer PCB workpiece, maintaining correct chip loads are of paramount importance, due to the fact that inadequate chip loads very often lead to poor hole quality and excessive tool wear or even unexpected tool breakage [7,8]. However, only limited research has investigated methods for an instrumented smart spindle to detect tool wear in application of high speed drilling.

The research work presented in this paper aims to develop an innovative method to prevent aerostatic bearings from being over-loaded, detect the engagement of each of copper layers in multilayer PCBs drilling, and most

importantly monitor tool wear applied to high speed drilling based on the unique feature of aerostatic bearing. The innovation is embodied with the development of an instrumented smart aerostatic bearing spindle for high speed PCB drilling. The development is industrial driven for coping with the ever increasing circuitry density and thus the smaller holes on the PCBs, while also demonstrates pursuing the industrial-feasible approach for high precision micro drilling, and future ultraprecision and micro machining.

2 Experimental setup

Experimental drilling trials have been carried out using an aerostatic bearing spindle with no external cooling applied to either the multilayer PCB workpiece or drilling tool. The commercial available spindle D1790 made from Westwind Air Bearing Ltd can provide a wide choice of spindle speed from 30 krpm up to 285 krpm within 5 μm dynamic runout in application of high speed drilling. Moreover, the outer thrust bearing plate of the spindle was equipped with an eddy current probe commercially available from Lion Precision Ltd. The aerostatic bearing spindle as shown in Fig. 1(a), the shaft is supported by two journal bearings fitted either side of a centrally mounted electrical motor, with a thrust bearing system (including an inner thrust bearing plate and an outer thrust bearing plate) located at one end of the shaft. In order to install the probe with a distance of 6 mm away from the shaft rotary axis, the outer thrust bearing plate has been modified by drilling a through hole as shown in Fig. 1(b). Moreover, it is extremely critical to ensure that the probe measurement face is flush with the outer thrust bearing face; otherwise, the cavity introduced could lead to a self-exciting instability sometimes called ‘air hammer’ to a thrust bearing. Furthermore, Fig. 1(b) also shows the axial shaft position with respect to an axial pushing or pulling forces measured from the probe in high speed drilling. So if the shaft deviates $-\Delta z$ from its natural position z towards the probe when an axial pushing force is applied and vice versa. The other, important issue needed to be addressed is that the temperature coefficient of the eddy current probe has a severe impact on both the precision and the repeatability of measurements in particular to micro machining application, when exposed to temperature variation. Therefore, both the probe and driver were chosen with a great care to provide a good temperature characteristic (the probe temperature drift from 15 °C to 65 °C: 0.01% F.S/°C and the driver temperature drift from 15 °C to 65 °C: 0.01% F.S/°C). Moreover, the temperatures of critical parts of the spindle (including the front and rear journal bearings as well as the inner and outer thrust bearings) are quite stable with water coolant applied. Particularly, when the cutting parameters are chosen as fixed values, the drift has been observed to be negligible for micro drilling. The spindle with built-in position measurement, called the instrumented smart spindle in this research, is used to measure axial shaft displacement (also known as the axial displacement).

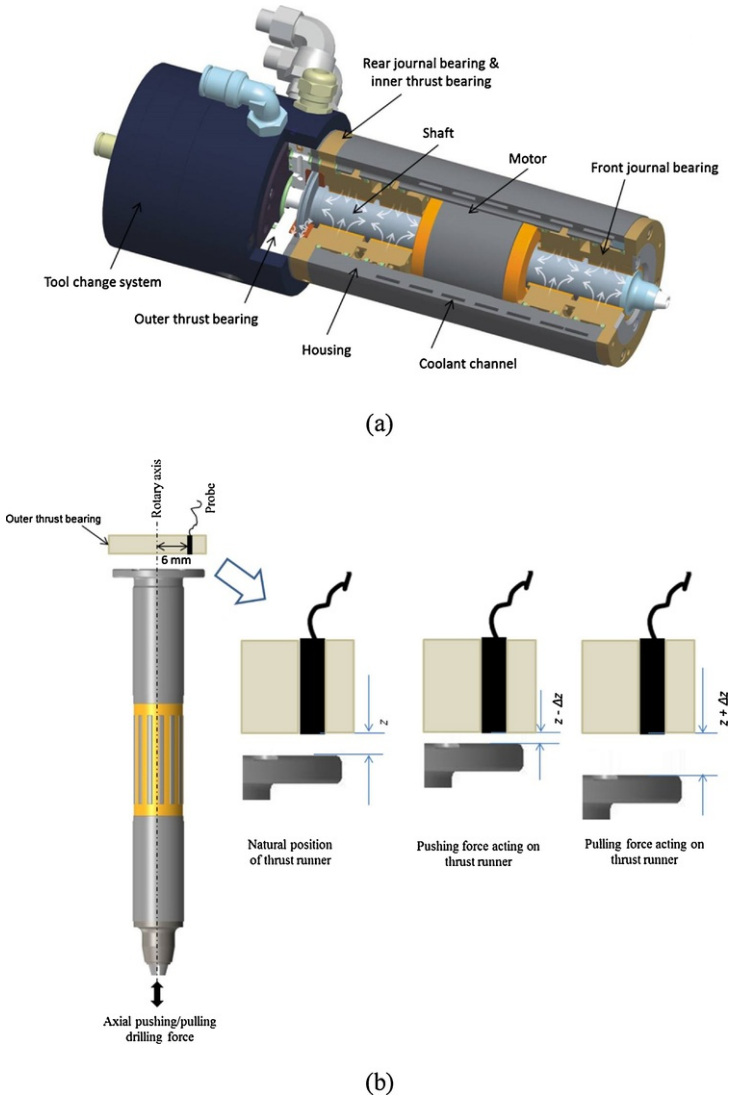

Fig. 1 (a) Schematic diagram of an aerostatic bearing spindle with the probe equipped with a distance of 6 mm from the shaft rotary axis; (b) the axial shaft position measured from the probe with respect to the axial pushing/pulling forces.

alt-text: Fig. 1

To measure both thrust forces and drilling torques in real time a Kistler dynamometer (9345A) was mounted on to the machine bed. The PCB workpiece was mechanically clamped down to the dynamometer with four screws. A drilling torque was developed when dual cutting flutes of a drill bit encounter a workpiece as the spindle feeds downward with a given feed-rate. The dynamometer was used to measure the corresponding reaction torque with built-in piezoelectric materials that can covert a mechanical stress into an electric charge. The real-time signals of both force measurement and shaft movement were collected into a PC via an NI 9237 data acquisition card (DAQ) controller by a bespoke program written in LabVIEW. The sampling frequency was 25.6 kHz and the size of each sample was 256 thousand points taken 10 s~~econds~~ in order to capture the full length of drilling process. Fig. 2 shows the detailed experimental setup technical specifications of the drilling system, including the micro drill, the Kistler dynamometer (9345A), the aerostatic bearing spindle and the eddy current probe.

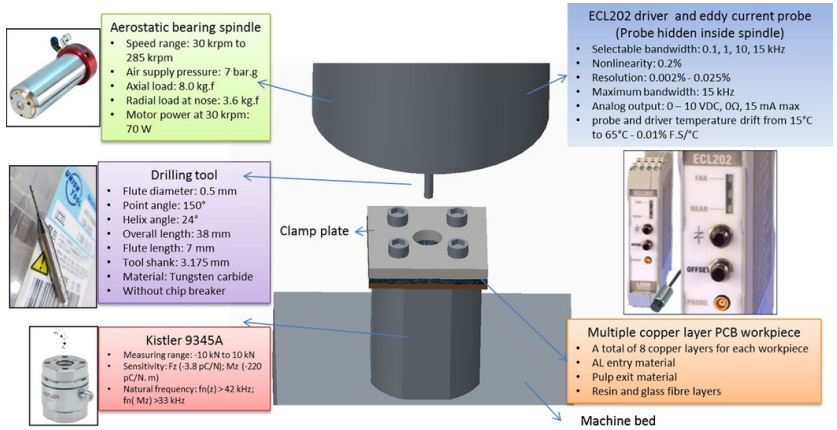

Fig. 2 Experimental setup of the high speed drilling system, including micro drill, Kistler dynamometer (9345A), aerostatic bearing spindle, and multilayer PCB workpiece.

alt-text: Fig. 2

The structure of the customized multilayer PCB workpiece consists of a constant thickness of seven glass fibre resin layers covered with copper layers of the different thicknesses as listed in Fig. 3. Moreover, an aluminium entry material (0.2 mm in thickness) and a pulp exit material (5 mm in thickness) were placed on both sides of PCB, as is common practice in high speed drilling. Furthermore, a constant feed was used to peck drill through each layer including the aluminium entry material, the copper and glass fibre resin layers, and the exit material.

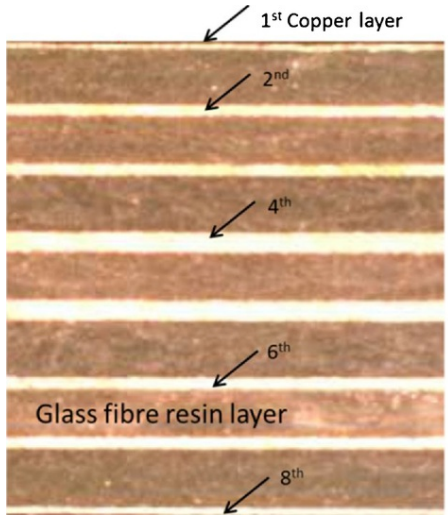

Multilayer PCB workpiece configuration

Copper layer Number	Thickness µm
1	17
2	35
3	35
4	70
5	70
6	35
7	35
8	17
Glass fibre resin layer	200

Fig. 3 Multilayer PCB workpiece configuration indicating the thickness of the copper layer and the glass fibre resin layer.

alt-text: Fig. 3

3 Results, analysis and discussion

3.1 Analysis of axial drilling force and drilling torque

Some preliminary trials were carried out on a single spindle drilling machine using drill size of 3 mm in diameter for peck drilling the customized multilayer PCB workpiece with a spindle speed of 30 krpm and feed-rate of 1.5 m/min. A program written in LabVIEW was used to obtain the axial drilling force, as shown in Fig. 4, and its corresponding frequency domain, as shown in Fig. 5. In Fig. 4, it is observed that the amplitudes of axial drilling force, to

some extent, are correlated with the thickness of the each of copper layers. The 1st peak corresponds to the engagement of the aluminium entry layer, the 2nd peak corresponds to the 17 µm thickness copper layer and the 4th and 5th peaks correspond to the 70 µm thickness copper layer. It is also be noted that the rising edges of the each of axial drilling forces are attributed to the fact that the copper layer is being pushed by the chisel edge of drilling tool, followed by the falling edges and high frequency oscillations (presented in two red boxes); the former is primarily due to cutting process occurrence and the latter is due to drilling through glass fibre resin layers. By applying Fast Fourier Transform (FFT) signal processing technique, extra information about the frequencies of axial drilling force are shown on the horizontal axis of Fig. 5, indicating that there are three dominant peaks. The 1st peak located in the frequency of 426 Hz called the fundamental frequency, equivalently to a spindle rotating speed of 25.56 krpm in this case, is generated primarily due to the residual rotor unbalanced mass. The 3rd peak located in the frequency of 855 Hz is twice the fundamental frequency, namely the second harmonic, generated due to dual cutting edges of the PCB drilling tool. The 2nd peak of 804 Hz is the thrust bearing resonant frequency of the spindle which can be accurately detect by impact hammer testing.

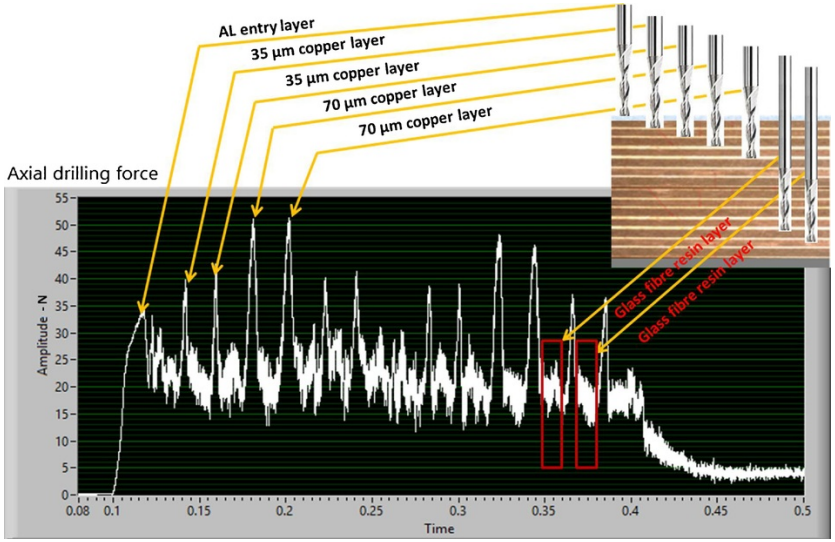

Fig. 4 A measure of axial drilling force while drilling through multilayer PCB workpiece (feed-rate of 1.5 m/min and spindle speed of 30 krpm).

alt-text: Fig. 4

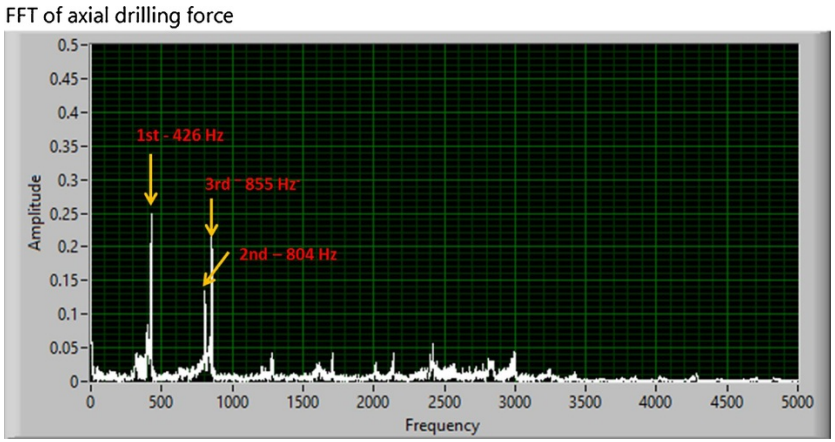

Fig. 5 Frequency domain of the axial drilling force after FFT conversion.

alt-text: Fig. 5

The torques transmitted from the drill cutting edge to the spindle shaft can vary dramatically during drilling the laminar form of the PCB material due to the fact that the primary cutting edge very often encounters more than one layer simultaneously, particularly with large diameter drill tools having relatively small point angles. In an extreme case, as shown in Fig. 6, the periphery of the primary cutting edge, represented as red, is cutting the aluminium entry material while the second part of the primary cutting edge, represented as green, is cutting the copper layer and, the rest as blue is cutting the glass fibre resin layer [9]. However, even in that complicated scenario, to some extent, a partial correlation between the axial drilling force and drilling torque still exists as shown in Fig. 7 (a), that is, when the peaks of axial drilling force including the rising edges, as highlighted in the red blocks, occur where the oscillation amplitudes of drilling torque are relatively small, because the mechanical push force developed from the chisel edge is more dominant than the cutting action developed from the two primary cutting edges [10]. Moreover, to explore the drilling torque represented in the yellow box further, it is divided into four moments as shown in Fig. 7 (b). The 1st moment demonstrates that the partial primary cutting edge adjacent to the chisel edge starts cutting the copper layer while the chisel edge engages with the glass fibre resin layer and the outer primary cutting edge cuts the glass fibre resin layer as well, which leads to a reduction in the amplitude of axial drilling force. As the drill feeds downward with a given feed-rate, the cutting engagement between the copper layer and the primary cutting edge shifts outwards (shown in the 2nd moment) until the periphery of the drill (shown in the 3rd moment), which leads to the oscillation amplitudes of the drilling torque slightly increasing, as shown in the yellow box of Fig. 7(a). The 4th moment demonstrates that the engagement length (ΔL_2) decreases compared to the ones (ΔL_1) that occurred in the previous moments, resulting to the oscillation amplitude of the drilling torque decreasing. Based on the basic engineering of torque concept, it is not difficult to realize that the greater drilling torque is reached when the outer primary cutting edges encounter the workpiece, in this case of combination of the copper and glass fibre resin layers, due to a larger distance measured from the force to the axis of shaft rotation. However, when the chisel edge fails to register with the aluminium entry layer, or even in the situations when the spindle dynamic runout is excessive, tool wear is severe, it is still extremely challenging to notice the partial correlation between the axial drilling force and drilling torque. Therefore, it is unlikely to explore further and find a correlation between the drilling torque and the multilayer PCB workpiece configuration.

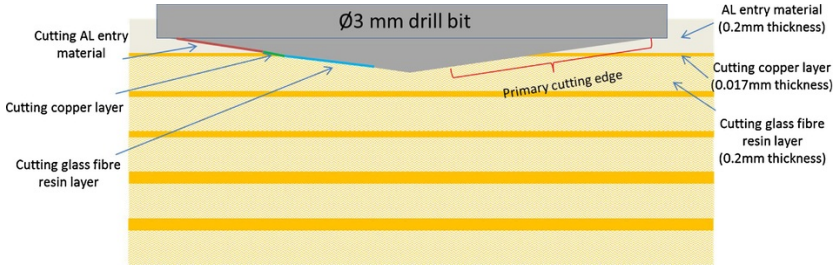

Fig. 6 Schematic diagram showing 3 mm diameter drill tool cutting the aluminium entry material, copper layer and glass fibre resin layer simultaneously.

alt-text: Fig. 6

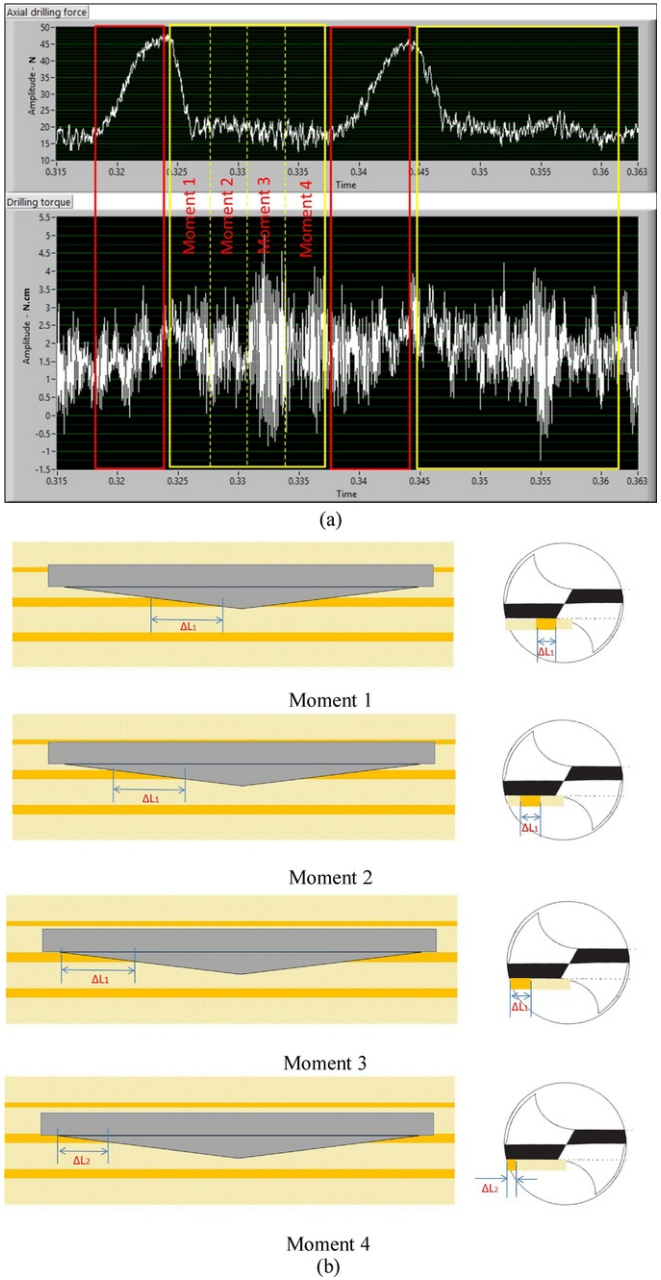

Fig. 7 (a) The axial drilling force and the corresponding drilling torque while drilling the 70 µm copper layer; (b) schematic diagrams divided into four moments demonstrating the engagement position and length between the primary cutting edge and copper layer.

alt-text: Fig. 7

3.2 Correlation of axial displacement and axial drilling force with respect to multilayer PCB workpiece configuration

Although there is the strong correlation between the axial drilling force and multilayer PCB workpiece configuration, force-based tool condition monitoring has not been well recognized in PCB drilling industry for two reasons; firstly the difficulty to establish an rigid workpiece/dynamometer mounting interface due to the PCB board size, as this can be several times larger than the physical size of the dynamometer, and secondly the frequency bandwidth and accuracy required for high speed drilling the dynamometer can be quite costly. So there is a need in the future to develop PCB drilling spindles with some built-in measurement feature, an instrumented smart spindle, in order to protect spindle as well as to detect tool wear. The axial drilling force and axial displacement were measured when peck drilling of the multilayer PCB workpiece with spindle of speed of 90 krpm and feed-rate of 1.6 m/min using a 0.5 mm diameter twist tungsten carbide drilling tool, as shown in Fig. 8 (a) and (b) respectively, in which both of the red waveforms represent raw signals and the white ones represent filtered signals with the low pass filter of 200 Hz applied. By implementing the 200 Hz low pass filter, both the squareness error and the form error are removed effectively, as well the surface roughness with respect to the spindle's thrust runner, because they are related to the fundamental frequency (426 Hz) or beyond. Furthermore, the filtered signals maintain their general trends and can still detect the engagements with each of the copper layers in particular; the latter, considered as one of critical features, is analysed in the following sections.

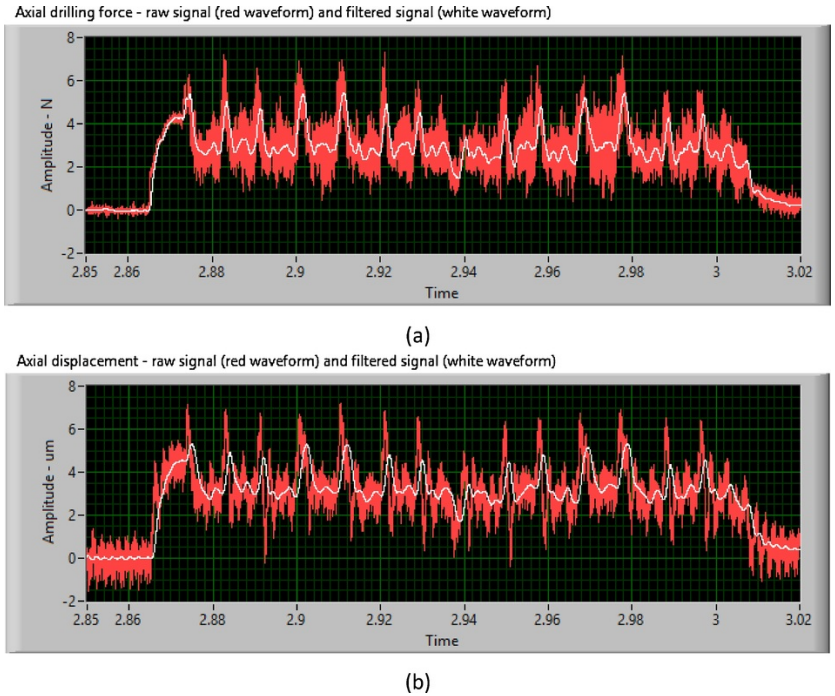

Fig. 8 A measure of (a) the axial drilling force and (b) the axial displacement. While drilling the multilayer PCB workpiece with 0.5 mm in diameter drilling tool, the red waveforms are the raw signal and the white waveforms are the filtered signal (feed-rate of 1.6 m/min and spindle speed of 90 krpm). (For interpretation of the references to colour in this figure legend, the reader is referred to the web version of this article.)

alt-text: Fig. 8

By applied a scale factor of 0.62 to the axial displacement, a comparison can be made between the filtered axial drilling force and axial displacement, shown in Fig. 9 (a). The maximum peaks displayed in the 4th, 5th, 10th and 11th in the sequence from the left hand side in Fig. 9 (a) is generated when the drill encounters the 70 μm thicknesses copper layers and the other peaks are related to the corresponding copper layers. Moreover, the Cosine matching method is adopted to investigate the waveform similarity, as given in the mathematical equation (1). All the points used to compose the filtered axial drilling force and axial displacement signals were put into the corresponding bins in terms of their amplitudes. Fig. 8 (b) shows the histograms of the axial drilling force (left hand side) and the axial displacement (right hand side) that contains a total number of 30 bins covering the signal amplitude range from 2 to 6 in the horizontal-axis and the corresponding percentage value of each bin as shown in the vertical-axis. Based on Equation (1), (1) and the percentage values provided in both of the histograms, the Cosine matching value is calculated to be 0.98 which implies the strong waveform similarity between the axial drilling force and axial displacement. It can be concluded that the instrumented smart spindle is capable of detecting each of the copper layers through measuring the axial displacement even with a 0.5 mm diameter drilling tool. With these results spindle protection and the PCB tool wear condition monitoring can be explored as a replacement for conventional force measurement based methods.

$$\cos(a) = \frac{\sum_{i=1}^{n} \vec{x}_i \times \sum_{i=1}^{n} \vec{y}_i}{\left|\sum_{i=1}^{n} x_i^2 \| \sum_{i=1}^{n} y_i^2\right|} \quad (1)$$

Where n is the number of bins, cos (αα) is the waveform similarity value, where x represents for the first waveform and y represents the second waveform.

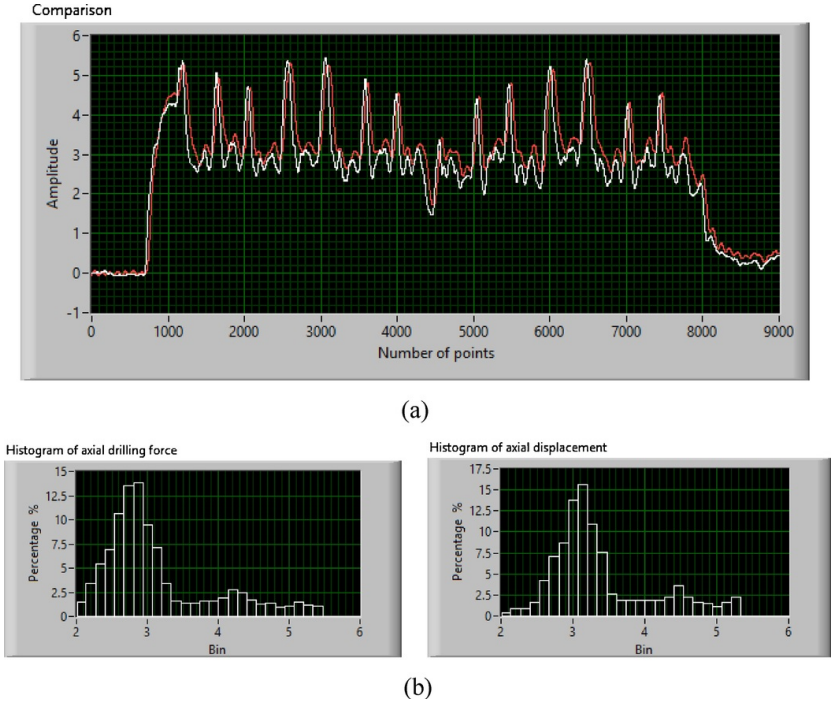

Fig. 9 (a) The comparison between the filtered axial drilling force (white waveform) and the filtered axial displacement (red waveform) with applied a scale factor of 0.62; (b) the histogram of the axial drilling force and the axial displacement for the Cosine matching calculation. (For interpretation of the references to colour in this figure legend, the reader is referred to the web version of this article.)

alt-text: Fig. 9

3.3 Spindle protection and drilling tool wear monitoring based on the axial shaft displacement

The instrumented smart spindle can provide an important feature of spindle protection, which is of paramount importance when drilling abrasive board materials like ceramic dielectric board and metal in board (MiB) in particular, because both of these boards will result in significant axial drilling forces acting on the spindle. Therefore, in order to achieve the significant drilling force and understand how it does affect the axial displacement, high feed-rate parameters are used in machining trials.

The preliminary cutting trials were carried out using drill size of 0.5 mm diameter, with a spindle speed of 90 krpm and feed-rate in the range from 1.6 to 3.6 m/min. Fig. 10 shows that the general trend of both the axial drilling forces and the corresponding axial displacements increase with the feed-rate. In particular, a relatively larger change occurred for both when the feed-rates increase from 2 m/min to 2.4 m/min, which could be due to the nonlinear effect of thrust bearing load capacity. Furthermore, the conclusion can be drawn that the instrumented smart spindle can be used for spindle protection, as the axial displacements generated while drilling, with high feed-rate parameters up to 3.6 m/mins in these preliminary cutting trials, were not even close to half of the designed air film clearance.

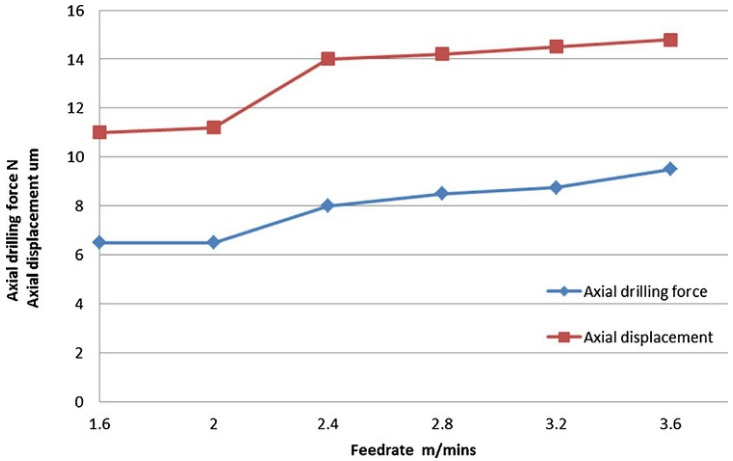

Fig. 10 The axial drilling force and axial displacement measured by the Kistler dynamometer and the instrumented smart spindle with a wide range of feed-rate parameters.

alt-text: Fig. 10

Fig. 11 shows the influence of the number of drilled holes on the axial displacement for three drill 0.5 mm diameter tools with feed-rate of 1.6 m/min and spindle speed of 90 krpm. The axial displacements were measured when the number of drilled holes reaches 500, 1000 and 1500, after measuring the first hole produced with a fresh drill. It is noticed that the axial displacement increases exponentially with the number of drilled holes and so a minimum axial movement of approximately 3.4 μm is achieved from the fresh drill and the maximum of 4.3 μm from the drill after 1500 holes. In addition, the axial displacement increases more significantly when drilling after 1500 holes compared to the drill after 1000 holes. Furthermore, the general trend in terms of the axial displacements produced the three drills with the different conditions are consistent, which was quite impressive due to a significant amount of debris produced in a real PCB drilling environment.

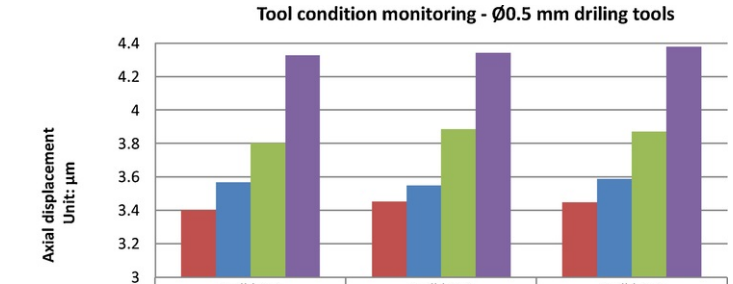

	Drill bit 1	Drill bit 2	Drill bit 3
Fresh drill	3.40168	3.45492	3.45012
Drilled 500 holes	3.56898	3.54893	3.58773
Drilled 1000 holes	3.80414	3.88653	3.87056
Drilled 1500 holes	4.32834	4.34247	4.38107

Fig. 11 The influence of the number of drilled holes on the axial displacement using three drilling tools of 0.5 mm in diameter (feed-rate = 1.6 m/min and spindle speed = 90 krpm).

alt-text: Fig. 11

Fig. 12 shows the progress of 0.5 mm diameter drilling tool wear with the number of drilled holes, resulting in the primary cutting edge to form into a 'butter knife shape' [11–13]. That means that the severest wear is observed to be on the periphery of the drilling tool and progressively decreasing to the centre, because the outer primary cutting edge experiences the greater torque than its adjacent ones. However, resin and glass fibre is found around the chisel edge region even after 1500 holes drilled, which would indicate that the drill is still capable of providing reasonable cutting rather than the passively forced cutting or even punching that can occur sin an extreme case, both of which can potentially generate an excessive cutting heat to melt the multilayer PCB workpiece [14]. Fig. 13 shows the influence of the number of drilled holes on burr formations formed on the top and bottom of copper layers

respectively. The burrs formed on the top copper layer is called entrance burr and on the bottom layer is called exit burr, however, both are based on different forming mechanisms. The entrance burr is formed into the interior of the hole via material plastic flow and the exit burr is formed into the exterior of the hole as material is mechanically pushed through the exit surface of the workpiece [15]. In Fig. 13, it is noticed that the number of drilled holes has little influence on the entrance burr but significantly affects the exit burr. When drilling the initial 500 holes, the exit burrs are not significant; however, they become more severe after 1000 holes drilled. Combining the above observations, the exit burrs are strongly influenced by the progress of drilling tool wear or, more specifically, the deterioration of the primary cutting edge, which leads to the greater axial drilling forces as well as the axial displacements. The latter, as shown in Fig. 11, demonstrates the increasing trend of the axial displacement with the number of drilled holes.

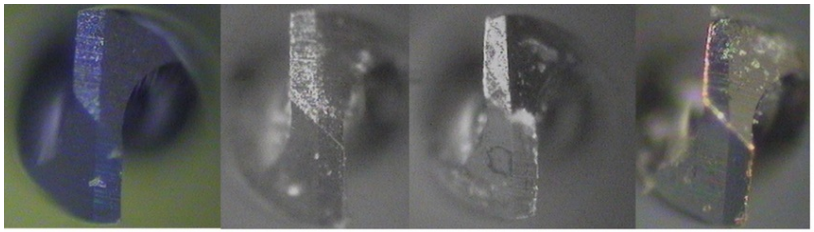

Fig. 12 The progress of drilling tool wear with the number of drilled holes (feed-rate = 1.6 m/min and spindle speed = 90 krpm).

alt-text: Fig. 12

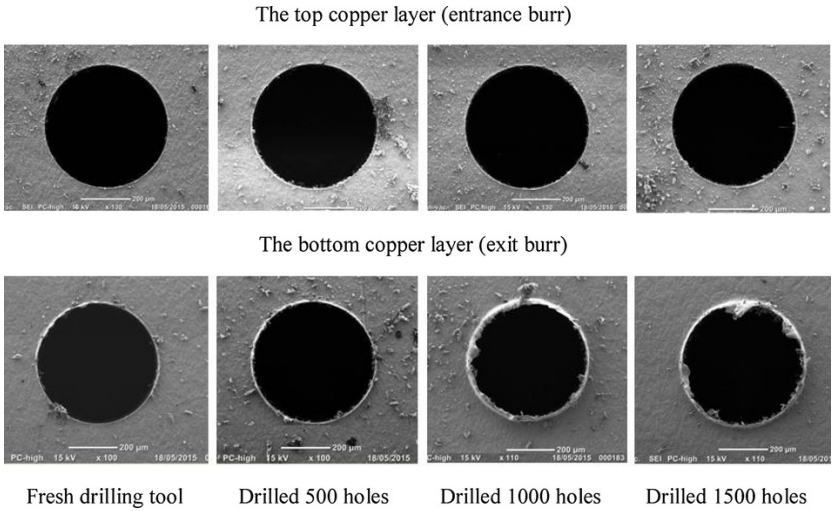

Fig. 13 SEM photos showing the influence of the number of drilled holes on the hole quality in terms of burr formation (feed-rate = 1.6 m/min and spindle speed = 90 krpm).

alt-text: Fig. 13

3.4 Nonlinear effect of thrust air bearing on the axial displacement measurement

In a typical modern PCB drilling spindle, the shaft will be supported by two radial bearings fitted either side of a centrally mounted electrical motor, with a thrust bearing system located at one end of the shaft. In almost all practical thrust bearings, the axial load capacity has a nonlinear relationship to the air film clearance. Fig. 14 shows the static test of the instrumented smart spindle, indicating the nonlinear relationship as expected between the axial load and axial displacement [16]. As a result, the last 15% of the axial displacement carries 44% of the total axial load capacity. Moreover, the instrumented smart spindle is capable of drilling a wide range of hole sizes on a variety of materials, requiring drill sizes from 1 or 4 mm in diameter to as small as 50 μm diameter. In Fig. 14, the total axial load of 73 N provided by the instrumented smart spindle is divided into three regions: A, B and C with the axial load in the range from 0 to 10 N, 11~~ to 32 N and 33 to~~ 32 N and 33 73 N, respectively. Furthermore, the drilling tools with the increased sizes are allocated to those three regions on which the drill sizes are ranged from 0.05 to 1 mm (Region A), 1~~ to~~ 3 mm (Region B), and 3~~ to~~ 4 mm (Region C), respectively, based on the axial load measurements by drilling the proposed PCB multilayer workpiece. By applying linear curve fitting to the three regions individually, the linear

equations and the corresponding R values are displayed in Fig. 14 indicating the reasonable fits with those curves. Most importantly, it is noticed that the constant of proportionality, also well known as stiffness in air bearing terminology, for each of the equations increases with the axial loads. That means that a reciprocal of those stiffness values, namely sensitivity in measurement terminology, decreases with the axial loads, that is, 1.19 applied to region A, 0.40 and 0.19 to region B and C respectively. Fortunately, a high sensitivity of 1.19 is kept within the most needed region where the relatively low axial drilling forces are normally produced due to small drill sizes. Alternatively, although the sensitivities drop by approximately 66% and 84% in both of regions B and C compared to the one in region A, the large axial drilling forces produced by large drill sizes can effectively compensate for it.

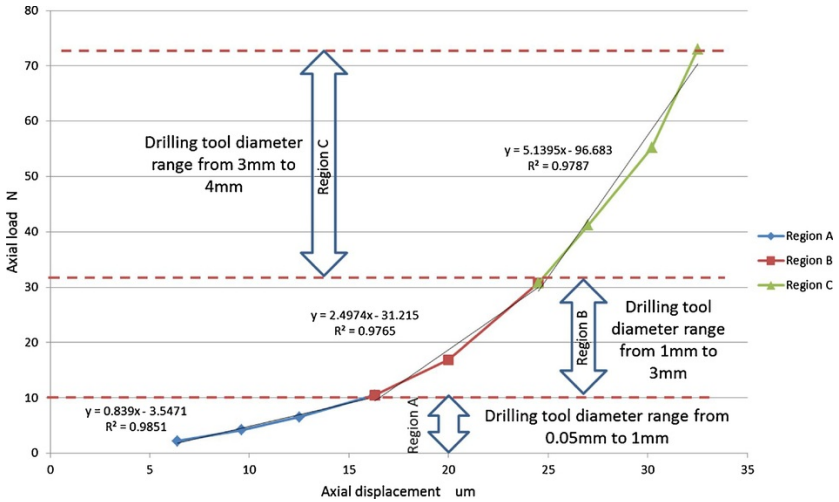

Fig. 14 The nonlinear relationship of the thrust bearing between the axial displacement and the axial load in the static test.

alt-text: Fig. 14

4 Conclusions

- The paper presents the experimental development of an instrumented smart spindle with application to high speed drilling of the multilayer PCB workpiece. The main findings and conclusions from this research can be summarized as follows:
- From the multilayer PCB workpiece machining trials, it is found that the amplitudes of axial drilling force are correlated with the thickness of the each of the copper layers. The critical frequency components in the frequency domain provide the evidence.
- A schematic diagram (as shown in Fig. 6), illustrates the engagement between the primary cutting edge and the different material layers simultaneously. A partial correlation is found between the axial drilling force and drilling torque as shown in Fig. 7(a) with the schematic diagrams explanations provided by four critical moments in Fig. 7(b). However, at this stage it is still a challenge to detect a correlation between the drilling torque and the multilayer PCB workpiece configuration.
- For a 0.5 mm diameter drilling tool, there is a strong correlation between the axial drilling force and the axial displacement by implementing 200 Hz low pass filter, as shown in Fig. 9(a), proven by the Cosine matching method (value of 0.98). Moreover, the instrumented smart spindle is capable of detecting each of copper layers through measuring the axial displacement.
- The instrumented smart spindle can perform the spindle self-protection, as demonstrated with the axial displacement measurement by implementing higher feed-rate parameters. The axial displacements generated in drilling with the given high feed-rate parameters up to 3.6 m/min were not even close to half of the designed air bearing film clearance.
- The instrumented smart spindle successfully detects and demonstrates the progress of drilling tool wear with the number of drilled holes based on the axial displacement measurements. The drilling tool wear is observed with the number of drilled holes, more specifically, the severest wear is detected to be on the periphery of the drilling tool and progressively decreasing to the centre because the outer primary cutting edge experiences the greater torque than its adjacent ones. Consequently, hole quality in terms of burr formation deteriorates with the number of drilled holes.
- The nonlinear effect of the thrust bearing has a strong influence on the sensitivities of the axial displacement measurements as illustrated in Fig. 14. However, the highest sensitivity is applied to region A for drilling tools with the relative small diameters, considered to be the most needed and important due to the low axial drilling forces. Although the sensitivity drops dramatically in both regions B and C, the large axial drilling forces produced by large drill sizes can effectively

compensate for the sensitivity loss.

Acknowledgements

This study was carried out within the scope of the collaborative research project between Brunel University London and Westwind Air Bearings Ltd, funded by the Innovate UK (KTP Contract No.: KTP009277). The authors acknowledge many useful discussions within the project team.

References

[1] E. Abele, Y. Altintas and C. Brecher, Machine ~~Tool Spindle UnitsCIRP Annals - Manufacturing Technology~~tool spindle units, *CIRP Ann Manuf Technol* **57**, 2010, 781–802.

[2] M.F. Chen, Y.P. Chen and C.D. Lin, Research on the ~~Arc Type Aerostatic Bearing for a PCB Drilling StationTribology International~~arc type aerostatic bearing for a PCB drilling station, *Tribol Int* **35**, 2002, 235–243.

[3] H.S. Yoon, J.S. Moon, M.Q. Pham, G.B. Lee and S.H. Ahn, Control of ~~Machining Parameters for Energy and Cost Savings in Micro-scale Drilling of PCBsJournal of Cleaner Production.~~machining parameters for energy and cost savings in micro-scale drilling of PCBs, *J Cleaner Prod* **54**, 2013, 41–48.

[4] C. Wang, K. Cheng and R. Rakowski, Design and ~~Analysis of a Piezoelectric Film Embedded Smart Cutting ToolProceedings of the Institution of Mechanical Engineering Part B Journal of Engineering Manufacturing~~analysis of a piezoelectric film embedded smart cutting tool, *Proc Inst Mech Eng Part B J Eng Manuf* **227**, 2012, 254–260.

[5] J.L. Stein and K. Huh, Monitoring ~~Cutting Forces in Turning: a Model Base ApproachJournal of Manufacturing Science and Engineeri~~cutting forces in turning: a model base approach, *J Manuf Sci Eng* **124**, 2002, 27–31.

[6] E. Dimla and S. Dimla, Sensor ~~Signals for Tool-Wear Monitoring in Metal Cutting Operations — a Review of MethodsInternational Journal of Machine Tools and Manufacturing~~signals for tool-wear monitoring in metal cutting operations –a review of methods, *Int J Mach Tools Manuf* **40**, 1999, 1073–1098.

[7] K. Cheng and D. Huo, Micro ~~Cutting: Fundamentals and A~~cutting: fundamentals and applications, 2013, John Wiley & Sons Ltd.

[8] L.J. Zheng, C.Y. Wang, L.P. Yang, Y.X. Song and L.Y. Fu, Characteristics of ~~Chip Formation in the Micro-drilling of Multi-Material SheetsInternation of Journal of Machine tools and Manufacturing.~~chip formation in the micro-drilling of multi-material sheets, *Int. J. Mach. Tools Manuf* **52**, 2012, 40–49.

[9] C. Wang, M. Wellstead, K. Cheng, D. Goodwin, J. Stratton and R. Rakowski, Overview the ~~Fundamental Issues in PCB Micro-Drilling I~~fundamental issues in PCB micro-Drilling industry, International conference on MicroManufacturing (4 M/ICOMM2015), Milan Italy, 2015.

[10] C. Wang, K. Cheng, R. Rakowski, D. Greenwood and J. Wale, Comparative ~~Studies on the Effect of Pilot Drillings with Application to High-speed Drilling of Carbon Fibre Reinforced Plastic (CFRP) CompositesInternational Journal of Advanced Manufacturing Technology1-~~studies on the effect of pilot drillings with application to high-speed drilling of carbon fibre reinforced plastic (CFRP) composites, *Int J Adv Manuf Technol* **1-13**, 2017, (online published).

[11] L.J. Zheng, C.Y. Wang, L.Y. Fu, L.P. Yang, Y.P. Qu and Y.X. Song, Wear ~~Mechanism of Micro-Drills during Dry High-Speed Drilling of PCBJournal of Materials Processing Technology.~~mechanism of micro-drills during dry high speed drilling of PCB, *J Mater Process Technol* **212**, 2012, 1989–1997.

[12] L.J. Zheng, C.Y. Wang, Y.P. Qu, Y.X. Song and L.Y. Fu, Interaction of ~~Cemented Carbide Micro-Drills and Printed Circuit Boards during Micro-drillingInternational Journal of Advanced Manufacturing Technology.~~cemented carbide micro-drills and printed circuit boards during micro-drilling, *Int J Adv Manuf Technol* **77**, 2014, 1305–1314.

[13] H. Watanabe, H. Tsuzaka and M. Masuda, Micro ~~Drilling for Printed Circuit Boards (PCBs)- Influence of Radial Run-out of Micro Drills on Hole QualityPrecision Engineering.~~drilling for printed circuit boards (PCBs)- influence of radial run-out of micro drills on hole quality, *Precis Eng* **32**, 2008, 329–335.

[14] M. Sato, T. Aoki, H. Tanaka and S. Takeda, Variation of ~~Temperature at the Bottom Surface of a Hole During Drilling and its Effect on Tool WearInternational Journal of Machine Tools and Manufacturing.~~temperature at the bottom surface of a hole during drilling and its effect on tool wear, *Int J Mach Tools Manuf* **68**, 2013, 40–47.

[15] B. Bhandari, Y.S. Hong, H.S. Yoon, J.S. Moon, M.Q. Pham, G.B. Lee, et al., ~~Y.C.HuangB.S.LinkeD.A.DornfeldDevelopment of a Micro-drilling Burr Control Chart for PCB DrillingPrecision Engineering.~~Development of a micro-drilling burr-control chart for PCB drilling, *Precis Eng* **38**, 2014, 221–229.

[16] M.F. Chen, W.L. Huang and Y.P. Chen, Design of the ~~Aerostatic Linear Guideway with a Passive Disk spring Compensator for PCB Drilling M~~aerostatic linear guideway with a passive disk-spring compensator for PCB drilling machining, *Tribol~~ogy International~~ Int* **43**, 2010, 395–403.

Queries and Answers

Query: The author names have been tagged as given names and surnames (surnames are highlighted in teal color). Please confirm if they have been identified correctly.
Answer: Yes

Query: "Your article is registered as a regular item and is being processed for inclusion in a regular issue of the journal. If this is NOT correct and your article belongs to a Special Issue/Collection please contact s.jayan@elsevier.com immediately prior to returning your corrections."
Answer: Yes, this article was submitted as a regular issue if the journal.

Query: One or more sponsor names and the sponsor country identifier may have been edited to a standard format that enables better searching and identification of your article. Please check and correct if necessary.
Answer: Yes

Query: Figs. 8,9 will appear in black and white in print and in color on the web. Based on this, the respective figure captions have been updated. Please check, and correct if necessary.
Answer: Yes, both figures are acceptable in B&W print